

Department of Physics and Astronomy  
University of Heidelberg

**Bachelor Thesis**

in Physics

submitted by

**Ole Schmidt**

born in Rendsburg, Germany

**2013**



# Characteristics of STDP on the Spikey neuromorphic hardware system

**This Bachelor Thesis has been carried out by Ole Schmidt at the**  
KIRCHHOFF INSTITUTE FOR PHYSICS  
RUPRECHT-KARLS-UNIVERSITÄT HEIDELBERG  
**under the supervision of**  
**Prof. Dr. Karlheinz Meier**



## Abstract

The goal of this thesis is a better understanding of the STDP mechanism on the Spikey chip. Existing measurement protocols for recording STDP curves are extended. It is now possible to record STDP curves with triples of spikes, which enhances the resolution of the curves. More detailed analysis of the recorded curves is possible by fitting exponential functions to the curves and determining amplitudes and time constants. With the objective of elongating the STDP time constants without the curves becoming asymmetric extensive parameter sweeps are performed. We were able to show that high time constants are reachable without adjusting the hardware parameter  $V_m$ , which controls the time constants by design. Furthermore, we determine the maximum limit of synaptic input rates to avoid saturation effects in the analog circuiting that lead to static synaptic weights.

## Kurzfassung

Ziel dieser Arbeit ist es, den auf dem Spikey Chip implementierten STDP Mechanismus besser zu verstehen. Hierzu werden bereits vorhandene Messprotokolle zur Aufnahme von STDP Kurven erweitert. Es ist nun möglich, STDP Kurven mit Tripeln von Aktionspotentialen aufzunehmen und so die Auflösung der Kurven zu verbessern. Durch das "Anpassen" einer Exponentialfunktion können Amplitude und Zeitkonstante bestimmt und somit die STDP Kurven genauer analysiert werden. Mit dem Ziel die STDP Zeitkonstanten zu verlängern, ohne dass die Kurven dabei asymmetrisch werden habe ich umfangreiche Messungen mit verschiedenen Sätzen von Parametern durchgeführt. Wir zeigen, dass hohe Zeitkonstanten möglich sind, ohne dabei den Hardware Parameter  $V_m$  zu benutzen, der nach dem Design des Chips die Zeitkonstanten kontrollieren sollte. Des weiteren ermitteln wir das maximale Limit für synaptische Input-Raten, um Effekte aufgrund von Saturation in den analogen Schaltkreisen zu vermeiden. Diese lassen die synaptischen Gewichte statisch werden.



# Contents

|          |  |           |
|----------|--|-----------|
| <b>1</b> | <b>Introduction</b>  | <b>1</b>  |
| 1.1      | Spike-Timing Dependent Plasticity . . . . .                            | 2         |
| 1.2      | Characteristic Features of the <b>Spikey</b> Chip . . . . .            | 3         |
| <b>2</b> | <b>Methods</b>   | <b>7</b>  |
| 2.1      | Recording of STDP Curves . . . . .                                     | 7         |
| 2.1.1    | Obtaining Accurate Spike Timing . . . . .                              | 8         |
| 2.1.2    | Recording STDP Curves with Spike Triples . . . . .                     | 8         |
| 2.2      | Analyzing the Effects of Hardware Parameters on STDP Time Constants .  | 10        |
| 2.3      | Determining the Capacities of Accumulating Spike Pair Events . . . . . | 11        |
| <b>3</b> | <b>Results</b>   | <b>13</b> |
| 3.1      | Recording STDP Curves with Spike Triples . . . . .                     | 13        |
| 3.2      | Effect of Hardware Parameters on STDP Time Constants . . . . .         | 14        |
| 3.3      | Determining the Capacities of Accumulating Spike Pair Events . . . . . | 19        |
| <b>4</b> | <b>Discussion and Outlook</b>  | <b>21</b> |
|          | <b>Bibliography</b>  | <b>26</b> |



# 1 Introduction

Synaptic plasticity is one of the key mechanisms for stabilizing large networks of neurons as there are for example in the human brain. A lot of experiments regarding synaptic plasticity are inspired by Hebb's postulate (*Gerstner and Kistler, 2002*):

*"When an Axon of cell A is near enough to excite cell B or repeatedly or persistently takes part in firing it, some growth process or metabolic change takes place in both cells such that A's efficiency, as one of the cells firing B, is increased"* (*Hebb, 1949*).

The proposition of the postulate is, in short, that cells that fire together, as a consequence wire together. But not only can the synapses be strengthened, but in terms of certain firing patterns they can also be weakened. It is believed that these persistent changes in the synaptic efficiency are corresponding to learning and memory on the scale of neural networks (*Gerstner and Kistler, 2002*). This study concentrates on Spike-Timing Dependent Plasticity (STDP) in which changes of synaptic weights are triggered by the timing of presynaptic action potential arrival and postsynaptic firing. It is a Hebbian-like learning rule on the level of individual action potentials (so called spikes). If the presynaptic spike arrives shortly before the postsynaptic neuron fires, the synapse is strengthened, because there might be a causal relation between these two events. On the other hand, the synapse is weakened, if the postsynaptic firing occurs shortly before a presynaptic spike, since there is an anti-causal relation between these events. Next to learning and memory on a large scale, STDP is also essential for signal transmission. One example is phase-locking (*Pfeil et al., 2013a*). Phase-locking enables temporal coding of signals with a precision much higher than the neuron's time constants would suggest (*Gerstner, 1996*). The high precision is only possible if synapses are "selected" that fire at a certain phase of the input signal. This is achieved by unsupervised STDP, which de-noises the input by strengthening these selected synapses. An application for phase-locking in biology is observed in the auditory pathway of barn owls (*Gerstner, 1996*). Phase-locked signal transmission enables very precise sound localization.

The goal of this thesis is to better understand the STDP mechanism on FACETS (*FACETS, 2010*) and BrainScaleS (*BrainScaleS, 2012*) neuromorphic hardware systems. During a preceding internship (*Schmidt, 2013*) STDP-curves were recorded using a simple network of 1 neuron that was connected to a source of action potentials representing the presynaptic neuron and some stimuli for triggering postsynaptic spikes. The network was implemented in PyNN (*Davison et al., 2008*) and simulated with NEST (*Gewaltig and Diesmann, 2007*). This thesis focuses on transferring the network onto the Spikey chip (*Schemmel et al., 2006; Pfeil et al., 2013b*) the aim being to do systematic measurements to search for parameters for phase-locking, e.g. a reasonable learning rate. The chip has specific synapse, neuron and plasticity models and limits on their configuration space not existent in software simulators. These limitations need to be taken into account. Next to

## 1 Introduction

the learning rate it has been tried to elongate STDP time constants to achieve a better ratio to the membrane time constant than there is in biology.

Getting a better understanding of the STDP mechanism on the **Spikey** chip is also of interest concerning the wafer-scale system, since a very similar mechanism is implemented on the HICANN chip (*Schemmel et al.*, 2010).

Earlier measurements of STDP as in *Müller* (2008), *Brüderle* (2009) or *Pfeil* (2011) are repeated systematically and the results are further evaluated especially with respect to the STDP time constants  $\tau_{\pm}$  and the learning rate, since these parameters are not easily adjustable.

### 1.1 Spike-Timing Dependent Plasticity

In this study, the time dependence of STDP will be treated as a pair-based update rule. There are different types of weight update rules for STDP that can be implemented on the **Spikey** chip, e.g. an additive weight update rule (*Song et al.*, 2000), a multiplicative weight update rule (*Turrigiano et al.*, 1998), mixtures of these (*Gütig et al.*, 2003), or a power law rule (*Morrison et al.*, 2007).

All measurements in this study use the additive weight update rule. Each time a postsynaptic spike propagates back to the synapse, the time difference  $\Delta t$  to the last occurrence of a presynaptic spike is measured. This is also done separately for each time a presynaptic spike reaches the synapse, the time  $\Delta t$  that has passed since the last postsynaptic spike being handled as a negative value. The STDP modification function  $F$  is defined as follows:

$$F(\Delta t) = \begin{cases} A_+ \exp(-\frac{\Delta t}{\tau_+}) & \text{if } \Delta t > 0 \text{ (causal)} \\ -A_- \exp(\frac{\Delta t}{\tau_-}) & \text{if } \Delta t < 0 \text{ (anti-causal)} \end{cases} \quad (1.1)$$

Adapted from *Song et al.* (2000), with the STDP time constants  $\tau_{\pm}$  for causal resp. anti-causal events. The parameters  $A_{\pm}$  scale the weight change.  $A_{\pm}$  is the maximum influence a single spike pair can have on the modification function (see Figure 1.1).

The synapse strength  $\omega$  changes depending on the STDP modification function  $F(\Delta t)$  and the previous strength  $\omega_{old}$  according to:

$$\omega_{new} = \omega_{old} \cdot (1 + F(\Delta t)) \quad (1.2)$$

Since only an additive weight update rule is used, there is no need for a weight dependence here. At the boundaries of the synaptic weight the new weight is just clipped to the border. These learning rules imply a change of the synaptic strength after each time a pair of pre- and postsynaptic spikes occurs. Due to limitations of the **Spikey** chip (the silicon area of the chip is finite and the weight update mechanism is implemented locally at every synapse) the weight resolution cannot be indefinitely accurate. Thus, a hybrid solution of digital and analog circuits is applied (see following Section 1.2).

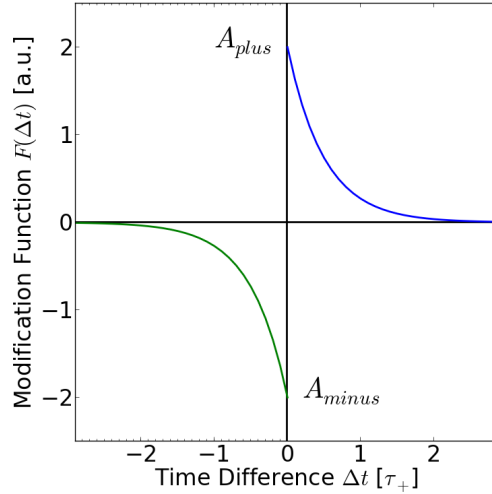


**Figure 1.1:** Schematic of an STDP modification function. The causal branch is drawn in blue, the anti-causal branch in green. The STDP modification function determines the time dependency of the weight modification. It consists of two exponentially decaying branches with the corresponding amplitudes  $A_+$  and  $A_-$  and the decaying time constants  $\tau_+$  and  $\tau_-$ . Adapted from *Brüderle* (2009).

## 1.2 Characteristic Features of the Spikey Chip

Owing to the limitations mentioned above, the **Spikey** chip only has a 4-bit synaptic weight resolution. This means there are 16 discrete values for the synaptic strength. A 4-bit weight resolution is not capable of considering every single spike pair for a weight update. But the information carried by a single spike pair should also not get lost. Hence, the information needs to be stored and only, if enough spike pairs occurred consecutively, the weight has to change. This is achieved by a setup sketched in Figure 1.2. Two capacitors, one for causal events and one for anti-causal events, are used for storing the information of each spike pair. The spike-timing dependent part (see Equation (1.1)) is implemented in the analog circuit of each synapse so that the charge loaded onto the corresponding capacitor decreases when the time between the two spikes  $\Delta t$  increases<sup>1</sup>. A digital controller periodically checks the capacitor voltages and performs a weight update once the difference of the two capacitors surpasses a certain threshold  $Q_{th}$ . If the capacitor collecting the causal events carries more charge than the capacitor collecting the anti-causal events the new weight is read from a look-up table  $LUT_c$  which holds new weights for every possible old value. For the anti-causal case, a second table  $LUT_a$  provides the new synaptic weight. For details see Table 1.1. Afterwards the voltages of the capacitors is reset to zero. The frequency with which the update controller checks

<sup>1</sup>Due to technical reasons the capacitors in the synapse circuits are charged at the beginning and then discharged until the threshold for a weight update is undershot. For easier descriptions it reads here that charge is brought onto the capacitors instead of taken away.

## 1 Introduction

| $\omega_{old}$ | $\omega_{new}$ | $\omega_{old}$ | $\omega_{new}$ |
|----------------|----------------|----------------|----------------|
| 0              | 1              | 0              | 0              |
| 1              | 2              | 1              | 0              |
| 2              | 3              | 2              | 1              |
| .              | .              | 3              | 2              |
| 14             | 15             | .              | .              |
| 15             | 15             | 15             | 14             |

LUT<sub>c</sub> (a)
LUT<sub>a</sub> (b)

**Table 1.1:** Look-up tables for causal weight changes (a) and anti-causal weight changes (b). The tables consist of 16 entries, one for every possible old synaptic weight.

the synapses depends on the number of synapses that are defined to be under STDP control. The number of those synapses can be controlled by a hardware parameter.

Previous measurements including STDP (*Pfeil et al.*, 2013a) suggest that with certain firing patterns it might be possible for the capacitors to fully charge without triggering a weight update. If there are alternating causal and anti-causal events transporting charge onto the capacitors they might fill up without their charge difference ever being large enough to cross the threshold  $Q_{th}$ . Quantifying how many spike pairs are necessary for inhibiting a weight update is another goal of this thesis. By progressively incrementing the number of alternating causal and anti-causal spike pairs before using only causal spike pairs (or anti-causal spike pairs resp.) for triggering a weight update the capacitance can be examined.

In Chapter 2 the methods are introduced in order to provide the basis for obtaining the results presented in Chapter 3. First of all, STDP curves are recorded with triples of spikes instead of pairs. More curves are recorded using different hardware parameter sets to analyze their impact on the STDP model parameters. At last, the capacitors are examined in detail. All results are discussed in Chapter 4 where also a short overview over the possible uses of the presented measurements in the future is given.

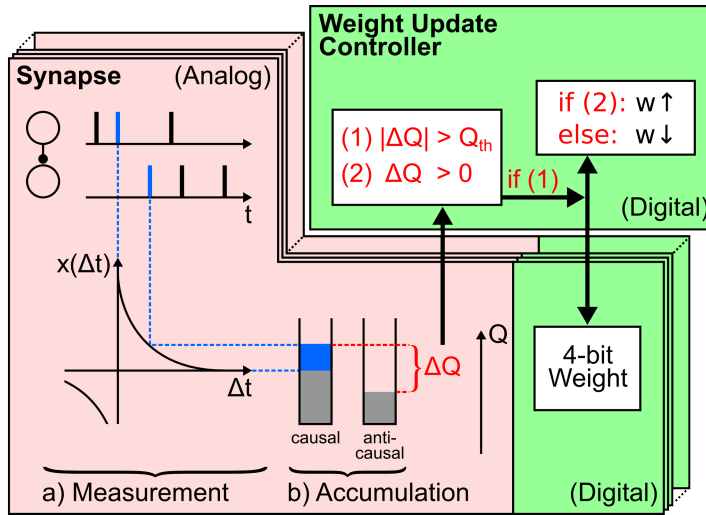


**Figure 1.2:** Sketch of the STDP mechanism implemented in every synapse on the Spikey chip. Analog circles are highlighted in red and digital circuits in green. The spike-timing dependence is **a)** measured and **b)** accumulated. In this sketch the capacitor collects a causal event since the presynaptic input reaches the synapse before the postsynaptic firing. The amount of charge depends on the time difference  $\Delta t$  between pre- and postsynaptic spikes (highlighted in blue, for more detailed information see text). When the weight update controller passes the synapse it evaluates whether the difference between the charges on the capacitors  $|\Delta Q|$  exceeds a configurable threshold  $Q_{th}$  (equation (1) from the figure). In that case the weight is increased if the charge on the capacitor storing causal events surpasses the charge of the capacitor storing anti-causal events. In the other case it is decreased (equation (2) from the figure). The new weight is retrieved from the LUTs according to the current weight and written back to the 4-bit digital weight storage of the hardware synapse. Adapted from Pfeil (2013).



## 2 Methods

The following chapter introduces the different methods that have been used to perform the measurements. At first, the network setup is presented which is used to record STDP curves (Section 2.1). The same setup is used to investigate the impact of hardware specific parameters on the STDP time constants (Section 2.2). Furthermore, the two capacities collecting causal and anti-causal events are sized in terms of spike pairs (Section 2.3). Using certain firing patterns one is able to determine how the capacitors might fully charge without eliciting a weight update and thus making the synaptic weights static.

### 2.1 Recording of STDP Curves

To acquire the STDP curves a simple network setup is used (see Figure 2.1a). Multiple synapses get the same presynaptic input to trigger a postsynaptic spike of a certain neuron. The observed synapse also connected to this neuron gets a different presynaptic input to induce a time difference  $\Delta t$  between this presynaptic input and postsynaptic firing.

A `Python` () script records the number of spike pairs necessary to induce a weight change for different  $\Delta t$ . If a weight update is not performed after  $N_{max} = 200$  pairs,  $N$  is set to  $N_{max}$ . The time between two subsequent spike pairs needs to be much higher than the STDP time constants  $\tau_{\pm}$  in order to keep the two branches with  $\Delta t < 0$  and  $\Delta t \geq 0$  of the STDP modification function (see Equation (1.1)) independent. So only causal spike pairs are accumulated on the capacitors, or anti-causal ones respectively. Since each spike pair with equal  $\Delta t$  delivers the same amount of charge onto one of the capacitors the number  $N$  of spike pairs necessary for surpassing the threshold  $Q_{th}$  and therefore triggering a weight update only depends on the time difference  $\Delta t$  between the two spikes:

$$Q_{th} \leq N \cdot \tilde{F}(\Delta t). \quad (2.1)$$

The tilde above the  $F$  in Equation (2.1) implies that the time dependency on the chip might not entirely match the STDP modification function (Equation (1.1)) due to hardware limitations.

The same script can be used to record STDP curves with triples of spikes instead of pairs (see Section 2.1.2) and to characterize the loading behavior of the capacities (see Section 2.3), only the timing of the spike trains needs to be adjusted. Since the exponential model of the STDP modification function (see Equation (1.1)) has been implemented in the hardware, an exponential correlation is expected between the time

## 2 Methods

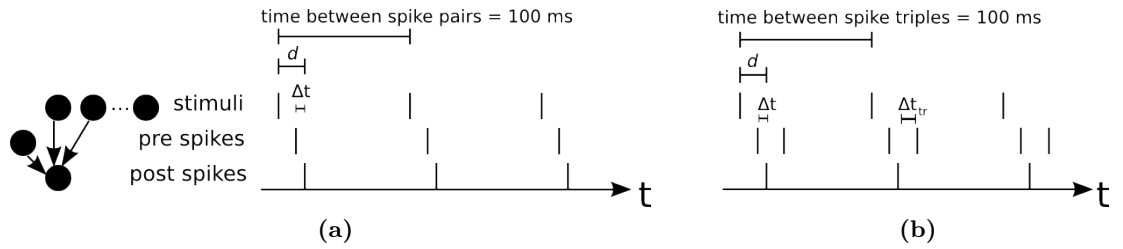


**Figure 2.1:** Timing of pre- and postsynaptic spiking. Several stimuli are connected to the postsynaptic neuron all firing at the same time to trigger postsynaptic firing after a certain delay  $d$ . A single observed synapse transmits the same spike train but shifted in time to induce a time difference  $\Delta t$  between presynaptic input and postsynaptic firing (a). Here three pairs of spikes are shown. In (b) the same setup is used but for each spike pair a third spike is added to the presynaptic spike train. Here three triples of spikes are shown.

difference  $\Delta t$  and the inverse of the number of spike pairs  $\frac{1}{N}$  that are needed for a weight update.

### 2.1.1 Obtaining Accurate Spike Timing

The presynaptic input can be set exact while the postsynaptic spikes need to be triggered by stimulating synapses all firing at the same time (see Figure 2.1). On hardware, the delay between triggering spikes and postsynaptic firing varies. A typical delay  $d = 2$  ms is used as initial value. After each experiment the actual delay between stimulus and postsynaptic firing is measured. If it deviates too much from  $d$ , the delay time is increased (or decreased resp.) and the last emulation run of the experiment repeated until the adjusted delay time matches the measured delay time within a certain precision ranging from 0.1 ms to 0.01 ms. That way the spike timing can be very accurate to the detriment of the total run time of the experiment.

To achieve a more regular postsynaptic firing, ten stimuli are applied to the neuron without adding presynaptic spikes at the plastic synapse. This way no weight modification is induced, since only pairs of pre- and postsynaptic spikes bring charge onto the capacitors collecting causal and anti-causal events.

Not every time the observed neuron is stimulated it emits a spike. Also without stimulation a spike can be emitted. In both cases the last emulation run will be repeated as well.

### 2.1.2 Recording STDP Curves with Spike Triples

One method developed in the preceding internship is the use of spike triples instead of pairs to record STDP curves. With very small time differences  $\Delta t$  between pre- and postsynaptic spiking, few spike pairs are sufficient to trigger a weight update. Since  $\Delta t$  is plotted over  $\frac{1}{N}$  and the measurement protocol only allows integers for  $N$ , plateaus occur in the range of small  $\Delta t$  (see Figure 2.3).

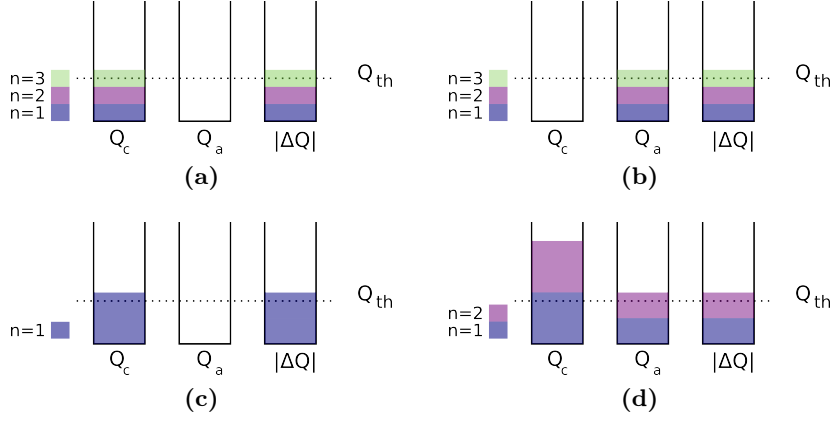


**Figure 2.2:** Sketch of different scenarios in which weight updates are triggered. In (a) and (b) a causal resp. anti-causal weight change is triggered by 3 spike pairs with a medium  $\Delta t$ . Since the time between the single spike pairs is large compared to  $\Delta t$ , only one capacitor is charged and therefore  $\Delta Q = Q_c \vee \Delta Q = Q_a$  applies. For smaller  $\Delta t$  one single spike pair can be sufficient to trigger a weight update (c). To circumvent a plateau  $N$  can be increased by using a third spike for charging both capacitors simultaneously (d). For more detailed information see Section 2.1.2.

As a weight update is only performed if the difference of the capacitor charges induced by causal and anti-causal spike pair events surpasses a certain threshold (see Section 1.2), the plateau can be avoided by bringing charge onto the technically unconcerned capacitor that should not collect any charge for single spike pairs. This is sketched in Figure 2.1b and Figure 2.2. Since the condition for a weight update is given by  $|\Delta Q| = |Q_c - Q_a| > Q_{th}$ , the threshold is not surpassed after a single spike pair if the synapse gets additional presynaptic input with time difference  $\Delta t_{tr}$  to the postsynaptic spike. For this purpose the following must apply:

$$\text{sgn}(\Delta t_{tr}) \neq \text{sgn}(\Delta t) \quad \text{and} \quad |\Delta t_{tr}| > |\Delta t| \quad \forall \Delta t. \quad (2.2)$$

The sign needs to be different so that the other capacitor gets charged. The time difference of the third spike must be larger, because otherwise the weight would change in the opposite direction. The spike trains are sketched in Figure 2.1b.

The amount of charge brought onto the capacitor with the third spike after  $\Delta t_{tr}$  is evaluated while recording the STDP-curve:

$$Q_{th} \leq N_{pairs} \cdot \tilde{F}(\Delta t_{tr}). \quad (2.3)$$

When triples of spikes are used to record STDP curves, for each data point the threshold  $Q_{th}$  is crossed by the difference of the two capacitors. In mathematical terms

$$Q_{th} \leq N_{tr} \cdot [\tilde{F}(\Delta t) - \tilde{F}(\Delta t_{tr})]. \quad (2.4)$$

Without the impact of the third spike the threshold would be crossed by

## 2 Methods

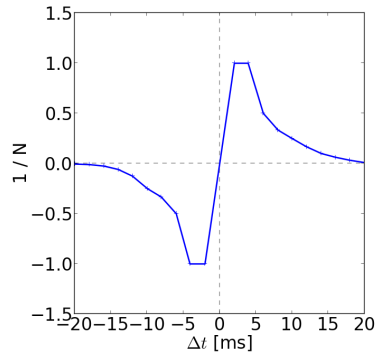


**Figure 2.3:** STDP curve recorded on the Spikey chip. The parameters were set in a way to illustrate the forming of a plateau in the region of  $|\Delta t| \leq 5$  ms. The inverse of the number of spike pairs  $N$  needed for a weight update is plotted over the time difference  $\Delta t$ .

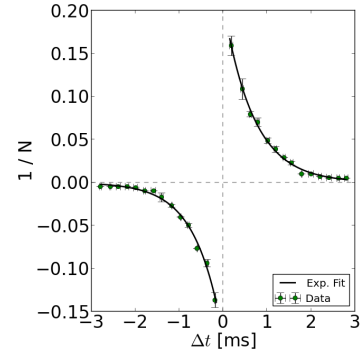


**Figure 2.4:** Exponential fit to data recorded with following parameters:  $V_m = 0$  V,  $V_{clrc} = V_{clra} = 0.95$  V,  $Q_{th} = 300$  mV (see footnote). This exemplary plot shows: it is feasible to plot an exponential function to the STDP curves.

$$Q_{th} \leq N_{theo} \cdot \tilde{F}(\Delta t). \quad (2.5)$$

These formulas can be used to convert the experimental results for  $N_{tr}$  into  $N_{theo}$  that would have been measured if only pairs of spikes were used. Equation (2.3) and Equation (2.5) are put in Equation (2.4). The solution is implemented in the data analysis:

$$\frac{1}{N_{theo}} = \frac{1}{N_{pairs}} + \frac{1}{N_{tr}}. \quad (2.6)$$

Notably, Equation (2.6) does not depend on the time modification function of the STDP model. Therefore, using triples of spikes is also applicable when a different time dependency is implemented. Note that  $\frac{1}{N}$  can be larger than 1 after the conversion.

## 2.2 Analyzing the Effects of Hardware Parameters on STDP Time Constants

There are different adjustable hardware parameters on the Spikey chip for the STDP mechanism. The threshold  $Q_{th}$  corresponds to the difference  $V_{cthigh} - V_{ctlow}$  with  $V_{cthigh}$  being the higher spike pair accumulation threshold and  $V_{ctlow}$  being the lower spike pair accumulation threshold<sup>1</sup>. The amount of charge that will be accumulated to the capacitor collecting causal or anti-causal events ( $Q_c$  or  $Q_a$ ) is controlled by the parameters  $V_{clrc}$

<sup>1</sup>For easier descriptions it is written that charge is accumulated to capacitors. On the Spikey chip the threshold  $Q_{th}$  is adjusted by two voltages. Hence, it is expressed in mV.

### 2.3 Determining the Capacities of Accumulating Spike Pair Events

and  $V_{clra}$ . The STDP time constants should by design be adjusted by the hardware parameter  $V_m$ . For a full overview of the hardware circuit used for implementing STDP see *Schemmel et al.* (2006).

STDP curves are recorded and analyzed using different sets of parameters. For each set the STDP time constants  $\tau_{\pm}$  and the amplitudes  $A_{\pm}$  are determined by fitting exponential functions to the two branches of the STDP curve.

$$f(x) = A_+ \exp\left(\frac{-\Delta t}{\tau_+}\right) \text{ for } \frac{1}{N} > 0 \quad (2.7)$$

$$f(x) = -A_- \exp\left(\frac{\Delta t}{\tau_-}\right) \text{ for } \frac{1}{N} < 0 \quad (2.8)$$

Since  $\frac{1}{N}$  is plotted over  $\Delta t$  one expects the amplitudes  $A_{\pm}$  to be connected to both the threshold and the amount of charge accumulated to the capacitors. The STDP time constants  $\tau_{\pm}$  should show a dependency on  $V_m$ .

The amplitudes and the time constants as well as the errors are determined by the least-squares method of the `Scipy.optimize` function. An exemplary exponential fit to a recorded STDP curve is shown in Figure 2.4. The data points are well described by the fit. Note that only the relative errors of the measured  $N$  are taken into account for the fits.

## 2.3 Determining the Capacities of Accumulating Spike Pair Events

Previous measurements on the *Spikey* chip suggested that the two capacitors collecting spike pair events might fill up under certain firing patterns without ever eliciting a weight update. An example is shown in Figure 2.5, where synapses adapt to a fixed input frequency. Compared to results in *Gerstner et al.* (1997), the synaptic weights do not split up between minimum and maximum value, but there are still synapses with medium weights left after the emulation on the *Spikey* chip.

By sending alternating causal and anti-causal spike pair events into the synapse the same amount of charge is accumulated onto both capacitors. After the alternating spike pair events loaded the capacitors, a second set of spike trains is injected to elicit a weight update. Quantifying the amount of charge necessary on both capacitors to inhibit a weight change can be done by consecutively increasing the number of alternating events until the weights become static. Then the capacitors are too small to accumulate enough charge from the second set of spike trains to surpass the threshold  $Q_{th}$ . The number of preloaded alternating events corresponds to the total amount of charge the capacitor is able to accumulate. An example for the timing of both sets of spike trains is depicted in Figure 2.6.

To ensure that the amount of charge accumulated to the capacitors is the same for causal and anti-causal events, first, STDP curves are recorded and analyzed. That way the values for  $\Delta t$  are determined separately for causal and anti-causal events since they may differ. For more detailed descriptions see Section 3.3.

## 2 Methods

Additionally, the experiments are done without the second set of spike trains. If the amount of charge accumulated to both capacitors is not equal as desired, a weight change will be induced. If the weight stays static it can be ruled out that a weight change is elicited by chance. This may happen because the spike times are not infinitely precise.

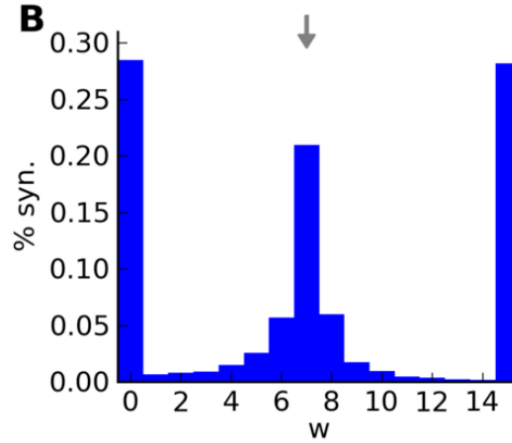


**Figure 2.5:** Distribution of synaptic weights after on-chip learning. All synapses receive the same input frequency. At the end of the emulation only strong synapses ( $w = 15$ ) or weak synapses ( $w = 0$ ) are expected. Against that expectation there are synapses left with medium weights. The arrow indicates the starting value ( $w = 7$ ) for the weights. Figure taken from Pfeil *et al.* (2013a).

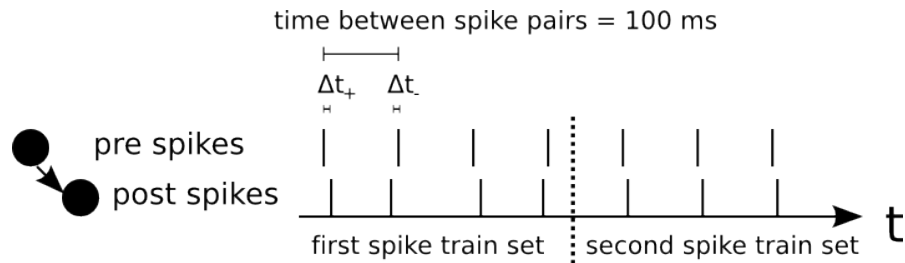


**Figure 2.6:** Timing of pre- and postsynaptic spiking, separated into two sets of spike trains. The first set loads the capacitors and the second set elicits a weight change. The stimulating spikes are omitted to simplify the sketch. In this example  $N_{charge} = 2$  alternating spike pairs load the capacitors and  $N = 3$  causal spike pairs elicit a weight update.

# 3 Results

## 3.1 Recording STDP Curves with Spike Triples

First, STDP curves have been recorded with spike pairs as described in Section 2.1 to experiment with different sets of parameters. For some parameters STDP curves show plateaus due to the measurement protocol described in Section 2.1.2. The curve is recorded once more with the same set of parameters, but with an additional third spike for  $|\Delta t| \leq 4.0$  ms. The use of a third spike enhances the resolution of the curves and narrows the plateaus (see Figure 3.1). The applied parameters are shown in Table 3.1.

The green curve in Figure 3.1 is computed from the red curve with Equation (2.6). It shows the results expected when only pairs of spikes are used. Therefore,  $N$  is not necessarily an integer anymore.

The method of using triples of spikes to enhance the resolution of STDP curves has been verified within a preceding internship (*Schmidt, 2013*). The recorded curves show the successful transformation of the measurement protocol with spike triples onto the Spikey chip.

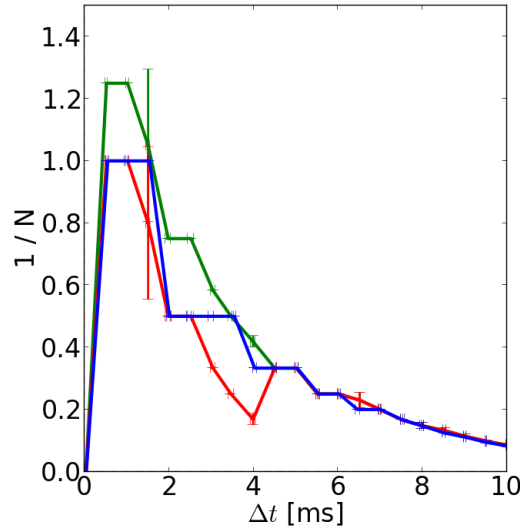


**Figure 3.1:** Comparison between STDP curves recorded with spike pairs (blue curve) and spike triples (green curve). Using an additional third spike, an improvement of the resolution of the curve is visible. The red curve shows the recorded data with triples of spikes before transformation with Equation (2.6). The data points and error-bars indicate the mean value and the standard deviation of 5 repetitive runs of the experiments. For better visualization only the causal branch is shown.

| Parameter                | Value            |
|--------------------------|------------------|
| $V_m$                    | 0 V              |
| $V_{cthigh}$             | 1 V              |
| $V_{ctlow}$              | 0.85 V           |
| $V_{clrc}$               | 1.24 V           |
| $V_{clra}$               | 1.22 V           |
| Range of $\Delta t$      | -10 ms ... 10 ms |
| Range of $\Delta t_{tr}$ | -4 ms ... 4 ms   |
| $\Delta t_{tr}$          | $\pm 6$ ms       |

**Table 3.1:** STDP parameters used for the curves in Figure 3.1.

### 3.2 Effect of Hardware Parameters on STDP Time Constants

The STDP time constants  $\tau_{\pm}$  can be adjusted by the hardware parameter  $V_m$ . To achieve a better ratio to the membrane time constant  $\tau_m$  as there is in biology ( $\frac{\tau_m}{\tau_{STDP}} \approx 1$ ) the STDP time constants need to be elongated. The higher  $V_m$ , the more  $\tau_{\pm}$  increase. The problem is that the STDP curves become very asymmetric for  $V_m > 0$  V. We are interested in the impact of other parameters on  $\tau_{\pm}$ ,  $A_{\pm}$  and the curve shape.

Hence, STDP curves are recorded with different values for the eligible hardware parameters  $V_{cthigh}$ ,  $V_{ctlow}$ ,  $V_{clrc}$  and  $V_{clra}$  mentioned in Section 2.2. The hardware is designed such that the working regime of the parameters is about 1 V to avoid unwanted hardware effects. Putting these parameters in Equation (2.1) and replacing  $V_{cthigh} - V_{ctlow}$  by  $Q_{th}$  results in:

$$Q_{th} \leq N \cdot V_{clrc/a} \cdot y(\Delta t, \dots) \cdot \exp\left(\frac{-|\Delta t|}{\tau_{\pm}}\right) \quad (3.1)$$

$$\implies \frac{1}{N} \leq \underbrace{\frac{V_{clrc/a} \cdot y(\Delta t, \dots)}{Q_{th}}}_{A_{\pm}} \cdot \exp\left(\frac{-|\Delta t|}{\tau_{\pm}}\right). \quad (3.2)$$

The amount of charge accumulated to the capacitors depends not only linearly on the parameters  $V_{clrc}$  and  $V_{clra}$ , but can be influenced by non-linear effects, expressed by  $y(\Delta t, \dots)$ . The non-linear effects have not been described yet. The effect of the threshold  $Q_{th}$  and the amount of charge accumulated to the capacitors via  $V_{clrc/a}$  on the STDP time constants  $\tau_{\pm}$  and the amplitudes  $A_{\pm}$  of the STDP curve are evaluated in the following.

All curves are recorded using the protocol described in Section 2.1 and only pairs of spikes are used. The experiments described in the next two Sections show that elongating  $\tau_{\pm}$  without distorting the shape of the STDP curves seems to be possible by adjusting the parameters  $V_{clrc/a}$  of the Spikey chip.

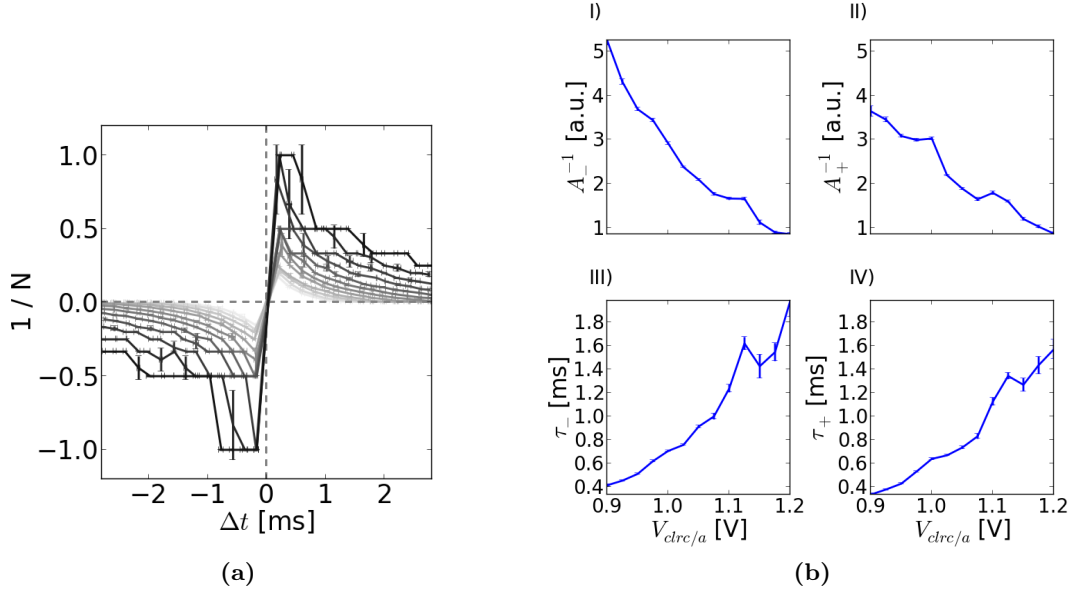


**Figure 3.2:** (a) STDP curves recorded sweeping over  $V_{clrc/a}$ . Darker curves indicate higher values for  $V_{clrc/a}$ . The data points and errorbars indicate mean value and standard deviation of 3 repetitive runs of the experiment. (b) Fit results for  $\tau_{\pm}$  and  $A_{\pm}$ . For  $0.9\text{ V} \leq V_{clrc/a} \leq 1.0\text{ V}$  there is already an increase of the time constants. The fit results for higher values of  $V_{clrc/a}$  are not reliable, because broad plateaus evolve and no reasonable fit can be done. Hence, only curves with  $V_{clrc/a} \leq 1.0\text{ V}$  are used for a more detailed characterization of the STDP mechanism.

### Sweep over $V_{clrc}$ and $V_{clra}$

First, the threshold is kept at  $V_{cthigh} - V_{ctlow} = 200\text{ mV}$  and a parameter sweep is performed over  $0.9\text{ V} \leq V_{clrc/a} \leq 1.2\text{ V}$ . For all experiments in this and the following Sections  $V_{clrc}$  and  $V_{clra}$  are kept equal, therefore only  $V_{clrc/a}$  is used from now on. The recorded STDP curves of the synapse in row 34 and column 4 of the chip<sup>1</sup> (synapse<sup>34x4</sup>) are shown in Figure 3.2a. An exponential function (see Equation (2.7)) has been fitted to all STDP curves. The fitting results can be seen in Figure 3.2b. The errorbars indicate the uncertainty of the fit. The inverse of the amplitude, which is the number of spike pairs  $N$  needed for a weight change with  $\Delta t = 0\text{ ms}$ , is plotted over  $V_{clrc/a}$ . For increasing  $V_{clrc/a}$  the inverse of the amplitudes  $A_{\pm}^{-1}$  decline almost linearly as expected from Equation (3.1). But also the time constants elongate. For  $V_{clrc/a} \leq 1.1\text{ V}$  the time constants both rise linearly and triple in the range of  $0.9\text{ V} \leq V_{clrc/a} \leq 1.1\text{ V}$ . For  $V_{clrc/a} \geq 1.1\text{ V}$  the fit results are not reliable since broad plateaus compose. Hence the outlier at  $V_{clrc/a} = 1.15\text{ V}$  is neglected. The curves are slightly asymmetric in the causal and anti-causal branch,

<sup>1</sup>The chip has one synapse block each on the left and on the right. Only the synapse block on the right is used for experiments in this study. Columns are counted from left to right, rows from bottom to top.

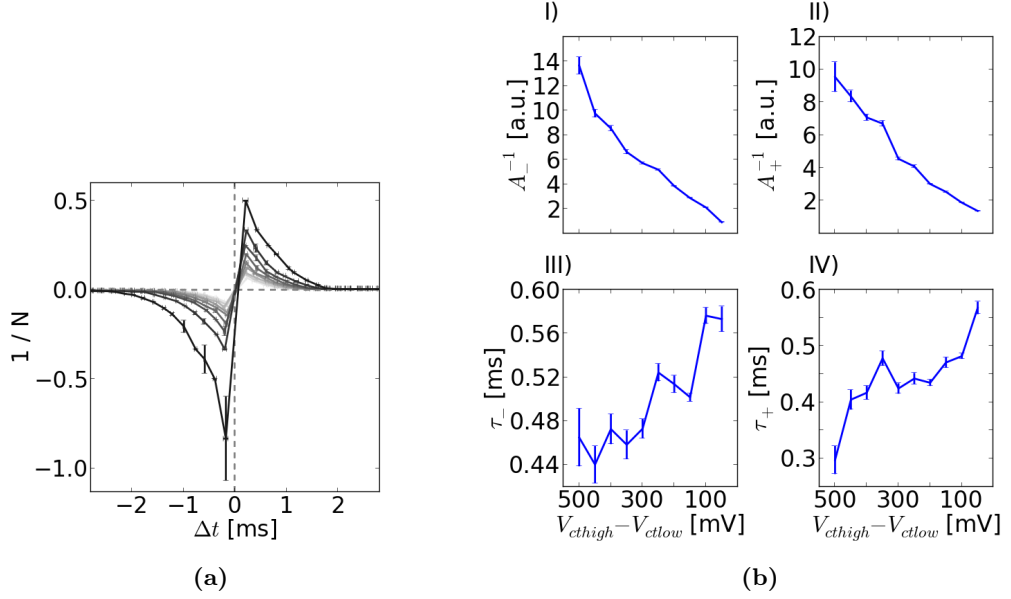


**Figure 3.3:** (a) STDP curves recorded sweeping over different thresholds.  $V_{cthigh} = 1.2$  V is held constant while  $V_{ctlow}$  is varied. Darker curves indicate higher values for  $V_{ctlow}$ , meaning a lower threshold. The data points and errorbars indicate mean value and standard deviation of 3 repetitive runs of the experiment. (b) Fit results for  $\tau_{\pm}$  and  $A_{\pm}$ . Consistent with Equation (3.1)  $A_{\pm}^{-1}$  declines linearly. Against expectations there is also a slight increase of the time constants for lower values of  $Q_{th}$  (see text for details).

therefore  $\tau_{-}$  is greater than  $\tau_{+}$ . This can best be seen in Figure 3.2a where the area under the darkest curve is larger for  $\Delta t < 0$  than for  $\Delta t > 0$ .

Since larger time constants are requested this effect of elongating time constants via  $V_{clrc/a}$  is evaluated more precisely (see Section 3.2).

### Sweep over the threshold $V_{cthigh} - V_{ctlow}$

In a next step,  $V_{clrc/a}$  are kept at 0.95 V and a parameter sweep is performed over the threshold:  $50 \text{ mV} \leq V_{cthigh} - V_{ctlow} \leq 500 \text{ mV}$ . The resulting curves can be seen in Figure 3.3a, their fit results in Figure 3.3b. For  $Q_{th} \leq 300 \text{ mV}$  the inverse of the amplitudes decline linearly whereas in higher threshold regime this is not clearly shown. Also the time constants elongate with a lower threshold, although this effect is not as strong as for  $V_{clrc/a}$ . For a decrease of the threshold by approximately 80% the time constants elongate by approx. 25% for  $\tau_{-}$  resp. approx. 75% for  $\tau_{+}$ . This is not described by Equation (3.1), where there is no dependency between  $Q_{th}$  or  $V_{clrc/a}$  on the time constants. The elongation via  $Q_{th}$  might change for different values of  $V_{clrc/a}$ . Recording curves with a threshold higher than 500 mV and doing an exponential fit is not feasible, because too many spike pairs are needed to induce a weight change.

### Closer Look on the Dependency of STDP Curves on the Parameters

To characterize the STDP mechanism, extensive parameter sweeps are done using only combinations of thresholds and values for  $V_{clrc/a}$  for which the fits of the STDP curves provide reasonable results. This means there are no plateaus and also enough data points with  $\frac{1}{N} > \frac{1}{N_{max}}$  so that fitting an exponential function to the data is possible without the errors for the fit parameters becoming too large. Hence, STDP curves are recorded with the parameters listed in Table 3.2.

To illustrate the results, the inverse of the fitted amplitudes and time constants are plotted as a function of  $Q_{th}$  and  $V_{clrc/a}$  (see Figure 3.4 - Figure 3.6). Darker fields correspond to less spike pairs needed for a weight change for  $\Delta t = 0$  ms, or longer time constants, respectively.

Since 25 STDP curves are recorded for each color plot and it takes about 18 minutes per curve, only three synapses were selected and analyzed: synapse<sup>4x4</sup>, synapse<sup>8x4</sup> and synapse<sup>34x4</sup>. Every data point represents the average of 3 measurements.

The same scales are used for the causal and the anti-causal branch of the STDP curves. This visualizes possible asymmetries in the different synapse circuits. The asymmetries exist due to production imperfections. For more detailed information see *Pfeil et al.* (2012).

For all synapses the time constants  $\tau_{\pm}$  as well as the amplitudes  $A_{\pm}$  increase<sup>2</sup> for higher values of  $V_{clrc/a}$  independently from the asymmetry within the synapse circuit. The asymmetry is strongest for the time constants of synapse<sup>8x4</sup>. For all sets of parameters  $\tau_{-}$  is shorter than  $\tau_{+}$ . The other synapses show slight asymmetries as well. For more detailed analysis of the asymmetric effects more synapses need to be evaluated. As expected from Figure 3.2b and Figure 3.3b, which show the cross section of the two dimensional plots, a lower threshold elongates the time constants, too.

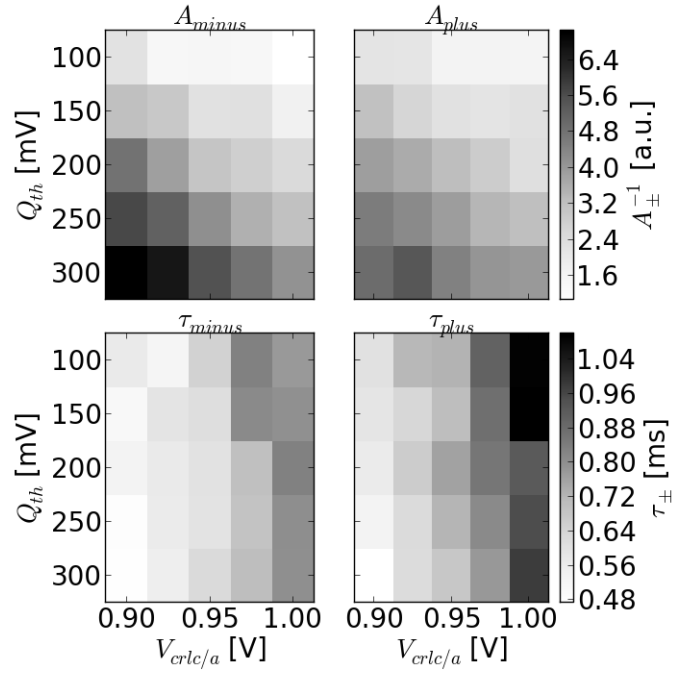
Figure 3.4 - Figure 3.6 show that elongating  $\tau_{\pm}$  is possible by simultaneously adjusting  $Q_{th}$  and  $V_{clrc/a}$ . The influence of  $V_{clrc/a}$  on the time constants is stronger than the influence of a lower threshold.

| Parameter               | Range             | Step size |
|-------------------------|-------------------|-----------|
| $V_m$                   | 0 V               | -         |
| $V_{cthigh}$            | 1.2 V             | -         |
| $V_{ctlow}$             | 0.9 V... 1.1 V    | 50 mV     |
| $V_{clrc}$ & $V_{clra}$ | 0.9 V... 1 V      | 25 mV     |
| $\Delta t$              | -3.0 ms... 3.0 ms | 0.2 ms    |

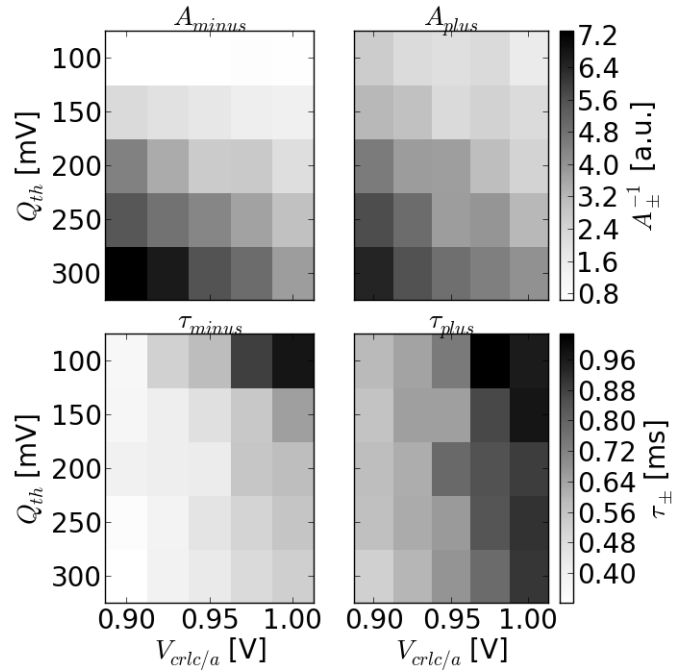
**Table 3.2:** STDP parameters used for the curves in Figure 3.4 - Figure 3.6

<sup>2</sup>Since the inverse of  $A_{\pm}$  is depicted, lighter colors correspond to higher amplitudes

**Figure 3.4:** Inverse of the amplitudes  $A_{\pm}$  and the time constants  $\tau_{\pm}$  of synapse<sup>4x4</sup> as a function of  $Q_{th}$  and  $V_{crlc/a}$ . Both amplitudes and time constants increase for higher values of  $V_{crlc/a}$  and for lower thresholds. Since the relative fit errors are all smaller than 2.2% of the fit results, they are not depicted here.



**Figure 3.5:** The same as in Figure 3.4 for synapse<sup>8x4</sup>.  $\tau_{+}$  is higher as  $\tau_{-}$  for all combinations of  $Q_{th}$  and  $V_{crlc/a}$ , indicating asymmetry in the synapse circuit. The errors for the fit results are about 4.3% of the fit result for  $V_{crlc/a} \geq 0.975$  V and  $Q_{th} = 100$  mV, for the other data points they can be neglected.



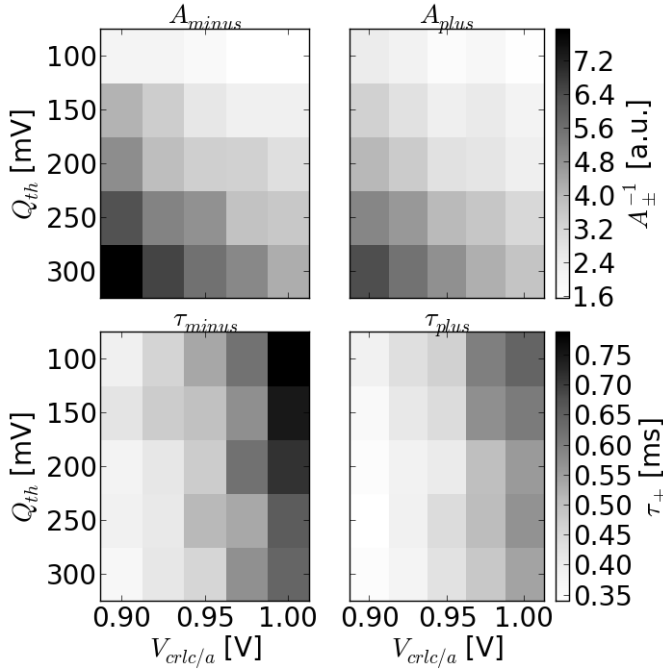


**Figure 3.6:** The same as in Figure 3.4 for synapse<sup>34x4</sup>. Only a slight asymmetry is visible. All relative errors are less than 2% of the fit results.

### 3.3 Determining the Capacities of Accumulating Spike Pair Events

A measurement protocol based on the descriptions in Section 2.3 is used to evaluate possible saturations of the capacitors. Instead of a single spike pair, always two spike pairs, one causal with time difference  $\Delta t_+$  and one anti-causal with time difference  $\Delta t_-$  are sent into the synapse.  $N_{charge}$  denotes the number of these alternating events. To make sure the amount of charge accumulated onto the capacitors is the same for both spike pairs, the fits of recorded STDP curves are used. First,  $\Delta t_+$  and  $\Delta t_-$  are determined by solving Equation (2.7) for a certain number of spike pairs  $N_{curve}$ :

$$\Delta t_- = -\tau_- \cdot \ln(N_{curve} \cdot A_-) \quad (3.3)$$

$$\Delta t_+ = \tau_+ \cdot \ln(N_{curve} \cdot A_+) \quad (3.4)$$

Second, choosing  $N_{charge} = 1$  as starting value,  $2 \cdot N_{charge}$  alternating pairs are accumulated onto the capacitors, followed by another  $10 \cdot N_{curve}$  non-alternating pairs to elicit a weight change. Ten times  $N_{curve}$  pairs are used to make sure the weight changes without the previous spike events.  $N_{curve}$  is incremented consecutively, until the synaptic weight stays static. Determining  $N_{curve}$  is repeated twice, one time causal events with time difference  $\Delta t_+$  are used to elicit a weight change and the other time anti-causal events with time difference  $\Delta t_-$  are used.

For example: the fits of STDP curves in Figure 2.4 are used. A causal weight change by  $N_{curve} = 10$  spike pairs results in a time difference between presynaptic spiking and postsynaptic firing of  $\Delta t_+ = 0.5$  ms. For an anti-causal weight change by  $N_{curve} = 10$

### 3 Results

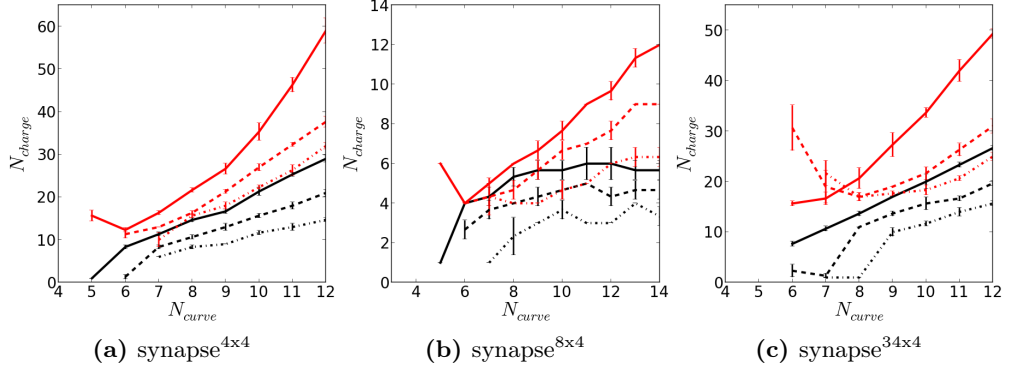


**Figure 3.7:** The number of pairs  $N_{charge}$  accumulated onto the capacitor until they saturate as a function of the number of spike pairs  $N_{curve}$  necessary to elicit a weight change. The curves are drawn red for an anti-causal weight change after loading the capacitors and black for a causal weight change. The dotted lines correspond to  $V_{clrca} = 0.925$  V, the dashed lines to  $V_{clrca} = 0.95$  V and the solid lines to  $V_{clrca} = 0.975$  V.

spike pairs, on the other hand, the time difference is  $\Delta t_- = -0.4$  ms. Then,  $2 \cdot N_{charge}$  spike pairs are sent into the synapse alternating with time difference  $\Delta t_+$  and  $\Delta t_-$ . If for  $N_{curve} \cdot 10$  subsequent causal spike pairs (or anti-causal ones, resp.) the weight stays static  $N_{charge}$  has been found. The capacitors are saturated.

$N_{charge}$  is plotted over  $N_{curve}$ , depicted for the same synapses as in Section 3.2 in Figure 3.7. The threshold is kept at  $Q_{th} = 300$  mV, while  $V_{clrca}$  are varied between 0.925 V and 0.975 V in 25 mV steps. That way the results from the previous Section 3.2 can be used to determine the necessary time differences  $\Delta t_-$  and  $\Delta t_+$ . If no suitable  $\Delta t_-$  or  $\Delta t_+$  for  $N_{curve}$  can be found, because with  $N_{curve}$  spike pairs no weight update can be elicited, the data point is omitted.

For higher values of  $N_{curve}$  less charge is accumulated onto the capacitors with each event. Hence,  $N_{charge}$  increases. For higher values of  $V_{clrca}$  the capacitors saturate slower. We did not expect differences in the curves for varied parameters, because these differences should be compensated by the fits for each individual STDP curve.

All red curves are higher than the green curves. Since a possible reason for this might be an asymmetry within the charging process ( $\Delta t_-$  might be too small and  $\Delta t_+$  too large or vice versa), the experiment is repeated without the second spike train. That means with only alternating causal and anti-causal events. A weight change is not elicited with  $N_{charge} = 250$  of such events. This shows that there is no asymmetry within the charging.

If no asymmetry in the charging process can be found, non-linear effects described by the factor  $y$  might explain the different results for causal and anti-causal weight change.

## 4 Discussion and Outlook

The analog characteristics of STDP on the **Spikey** chip could be analyzed for selected synapses. Although only three synapses were used, the tendencies were clearly visible.

**Higher resolution of STDP curves** Gathering more detailed information from the learning curves is possible by using additional presynaptic spikes as described in Section 3.1. Plateaus occur, if in the range of small  $\Delta t$  few spike pairs elicit a weight update. Hence, the number of spike pairs  $N$  for a different  $\Delta t$  may be the same, although the amount of charge accumulated to the capacitors differs. The information about the curve in the range of small  $\Delta t$  can now be resolved and does not necessarily get lost due to the measurement protocol (see Figure 3.1).

A disadvantage is the need to manually adjust the range of  $\Delta t$  in which the third spike is applied  $\Delta t_{tr}^{range}$  and the time difference  $\Delta t_{tr}$  of the third spike. Asymmetry in the synapses make it difficult to automatically determine these parameters. The optimal parameters were found by trial and error.

The resolution only improves in the range where a third spike is applied. No wide range can be chosen, because  $\Delta t_{tr}$  needs to be higher than  $\Delta t$  for all values in  $\Delta t_{tr}^{range}$  (Equation (2.2)). Since  $\Delta t_{tr}$  is constant its influence vanishes for a too wide  $\Delta t_{tr}^{range}$  for time differences close to zero.

It is not feasible to choose a variable  $\Delta t_{tr}$  due to error propagation. Small errors in calculating  $N_{theo}$  for large time differences propagate, since the calculated  $N_{theo}$  is used again to calculate the next  $N_{theo}$  for a smaller time difference and so on.

In all other parts of this study, only pairs of spikes are used for the measurements.

**Elongate time constants** Elongating the STDP time constants  $\tau_{\pm}$  is not only possible by adjusting the hardware parameter  $V_m$ , but also by increasing  $V_{clrc}$  and  $V_{clra}$ . The threshold  $Q_{th}$  has an influence on the time constants, too. Higher thresholds are connected to lower time constants. Since this effect is smaller than the influence of  $V_{clrc/a}$  (compare Figure 3.2b and Figure 3.3b), very high time constants can be achieved by choosing high values for  $V_{clrc/a}$  and a high threshold (see Figure 4.1). Time constants of  $\tau_- = 7.84(21)$  ms and  $\tau_+ = 6.68(19)$  ms could be achieved with the parameters listed in Table 4.1. The high threshold circumvents the occurrence of plateaus whereas the time constants elongate via  $V_{clrc/a}$ .

The two dimensional color plots in Section 3.2 show the dependency of  $\tau_{\pm}$  and  $A_{\pm}$  on the hardware parameters. They visualize that the information obtained by the parameter sweeps in Figure 3.2b and Figure 3.3b is also applicable for different values of  $Q_{th}$ , or  $V_{clrc/a}$  respectively.

## 4 Discussion and Outlook

As a consequence drawn from Section 3.2 time constants can better be elongated by increasing  $Q_{th}$  and  $V_{clrc/a}$  than  $V_m$  to avoid interference of  $y(\Delta t, \dots)$ .

**Optimal learning rate** In Section 3.3 it is shown that the capacitors collecting causal and anti-causal events can saturate and prevent the synapse to change its weight. This explains the static weights in *Pfeil et al.* (2013a) shown in Figure 2.5.

With the provided script it is now possible to estimate the optimal learning rate depending on the given model. This means the number of synapses defined to be under STDP control, the firing rate of the connected neurons or other spike sources and their correlations need to be known.

The more synapses are under STDP control the lower the frequency of the weight update controller. Given the frequency of the weight update controller the input rates and their temporal correlation should not drive the capacitors into the regime where they might saturate. Depending on the temporal correlation between the spikes, different numbers of alternating spike pairs might prevent the synapse to change its weight.

The ratio  $\frac{N_{charge}}{N_{curve}}$  varies for the analyzed synapses. For synapse<sup>8x4</sup> the ratio is close to one, which means that the synapse can become static very fast.

Figure 3.7 shows that the higher  $V_{clrc/a}$ , the higher the ratio  $\frac{N_{charge}}{N_{curve}}$ . In other words, the capacitors saturate slower for higher values of  $V_{clrc/a}$ . This effect is unexpected, because although  $V_{clrc/a}$  differ, the amount of charge accumulated onto the capacitors should not. To prevent this,  $\Delta t_-$  and  $\Delta t_+$  are determined for each value of  $N_{curve}$  and  $V_{clrc/a}$  as described in Equation (3.3). Although no suitable explanation could be found, the experiments show that increasing  $V_{clrc/a}$  can prevent saturation as well. Different ratios of  $\frac{N_{charge}}{N_{curve}}$  for causal and anti-causal weight change after loading the capacitors might be explained by non-linear effects. More detailed analysis of this matter go beyond the constraints of this study.

In accordance with the results from the parameter sweeps, it is recommended to adjust as high values for  $V_{clrc/a}$  as possible to elongate  $\tau_{\pm}$  and simultaneously prevent the capacitors from saturation.

For future experiments the measurement protocol as well as the results can be helpful, because the analog circuits of the STDP mechanism on the **Spikey** chip are the same as in the HICANN chip.

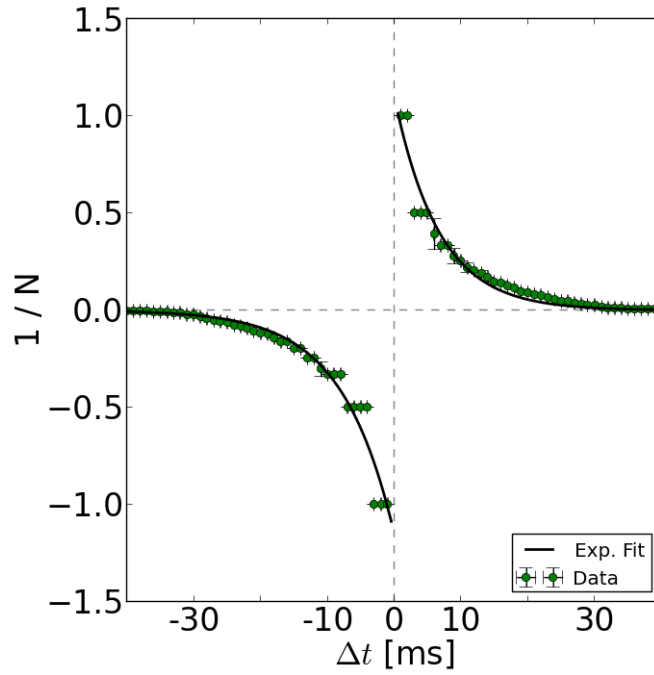


**Figure 4.1:** Elongating  $\tau_{\pm}$  without tuning  $V_m$  using the parameters listed in Table 4.1. Data points and error bars represent mean value and standard deviation of 3 repetitive experiment runs. The exponential fit yields  $\tau_- = 7.84(21)$  ms and  $\tau_+ = 6.68(19)$  ms. A slight deviation of the data points from the fit is visible. This is also an indicator for a superposition of the exponential function with another non-linear function.

| Parameter           | Value            |
|---------------------|------------------|
| $V_m$               | 0 V              |
| $V_{cthigh}$        | 1.2 V            |
| $V_{ctlow}$         | 0.8 V            |
| $V_{clrc}$          | 1.34 V           |
| $V_{clra}$          | 1.34 V           |
| Range of $\Delta t$ | -40 ms ... 40 ms |

**Table 4.1:** STDP parameters used for the curves in Figure 4.1.



# Bibliography

- BrainScaleS, Research, <http://brainscales.kip.uni-heidelberg.de/public/index.html>, 2012.
- Brüderle, D., Neuroscientific modeling with a mixed-signal vlsi hardware system, Ph.D. thesis, Ruprecht-Karls-Universität Heidelberg, 2009.
- Davison, A. P., D. Brüderle, J. Eppler, J. Kremkow, E. Müller, D. Pecevski, L. Perinet, and P. Yger, PyNN: a common interface for neuronal network simulators, *Front. Neuroinform.*, 2(11), 2008.
- FACETS, Research, <http://http://facets.kip.uni-heidelberg.de/>, 2010.
- Gerstner, W., A neuronal learning rule for sub-millisecond temporal coding, *Nature*, 383, 76–78, 1996.
- Gerstner, W., and W. Kistler, *Spiking Neuron Models: Single Neurons, Populations, Plasticity*, Cambridge University Press, 2002.
- Gerstner, W., R. Kempter, J. L. van Hemmen, and H. Wagner, A developmental learning rule for coincidence tuning in the barn owl auditory system, *Computational Neuroscience: trends in research, 1997*, 665–669, 1997.
- Gewaltig, M.-O., and M. Diesmann, NEST (NEural Simulation Tool), *Scholarpedia*, 2(4), 1430, 2007.
- Gütig, R., R. Aharonov, S. Rotter, and H. Sompolinsky, Learning input correlations through nonlinear temporally asymmetric hebbian plasticity, *The Journal of Neuroscience*, 23(9), 3697–3714, 2003.
- Hebb, D. O., *The Organization of Behaviour*, Wiley, New York, 1949.
- Morrison, A., A. Aertsen, and M. Diesmann, Spike-Timing-Dependent Plasticity in Balanced Random Networks, *Neural Comp.*, 19(6), 1437–1467, 2007.
- Müller, E., Operation of an imperfect neuromorphic hardware device, Diploma thesis, Ruprecht-Karls-Universität Heidelberg, hD-KIP-08-43, 2008.
- Pfeil, T., Configuration strategies for neurons and synaptic learning in large-scale neuromorphic hardware systems, Diploma thesis (English), University of Heidelberg, HD-KIP 11-34, 2011.
- Pfeil, T., personal communication, 2013.

- Pfeil, T., T. C. Potjans, S. Schrader, W. Potjans, J. Schemmel, M. Diesmann, and K. Meier, Is a 4-bit synaptic weight resolution enough? – Constraints on enabling spike-timing dependent plasticity in neuromorphic hardware, *ArXiv e-prints*, 2012.
- Pfeil, T., A.-C. Scherzer, J. Schemmel, and K. Meier, Neuromorphic learning towards nano second precision, *arXiv preprint arXiv:1309.4283*, 2013a.
- Pfeil, T., et al., Six networks on a universal neuromorphic computing substrate, *Frontiers in Neuroscience*, 7, 11, doi:10.3389/fnins.2013.00011, 2013b.
- Python, *The Python Programming Language*, Python Software Foundation, [Online; accessed: 2014-04-29], 2014.
- Schemmel, J., A. Grübl, K. Meier, and E. Muller, Implementing synaptic plasticity in a VLSI spiking neural network model, in *Proceedings of the 2006 International Joint Conference on Neural Networks (IJCNN)*, IEEE Press, 2006.
- Schemmel, J., A. Grübl, and S. Millner, Specification of the HICANN microchip, FACETS project internal documentation, 2010.
- Schmidt, M. O., Aufnahme von STDP-Kurven mit Tripeln von Aktionspotentialen, Internship Report (German), University of Heidelberg, HD-KIP 10-43, 2013.
- Song, S., K. Miller, and L. Abbott, Competitive hebbian learning through spiketiming-dependent synaptic plasticity, *Nat. Neurosci.*, 3, 919–926, 2000.
- Turrigiano, G. G., K. R. Leslie, N. S. Desai, L. C. Rutherford, and S. B. Nelson, Activity-dependent scaling of quantal amplitude in neocortical neurons, *Nature*, 391, 892–896, 1998.

## Statement of Originality (Erklärung):

I certify that this thesis, and the research to which it refers, are the product of my own work. Any ideas or quotations from the work of other people, published or otherwise, are fully acknowledged in accordance with the standard referencing practices of the discipline.

Ich versichere, dass ich diese Arbeit selbständig verfasst und keine anderen als die angegebenen Quellen und Hilfsmittel benutzt habe.

Heidelberg, May 6, 2014

.....  
(signature)